Management and Production Engineering Review
Volume 6 • Number 4 • December 2015 • pp. 43–54
DOI: 10.1515/mper-2015-0035

DE GRUYTER OPEN

mper

LASER NANOSOLDERING OF GOLDEN AND MAGNETITE PARTICLES AND ITS POSSIBLE APPLICATION IN 3D PRINTING DEVICES AND FOUR-VALUED NON-VOLATILE MEMORIES

Jacek Jaworski[1], Grzegorz Gawłowski[2]

[1] *Polish Academy of Sciences, The Henryk Niewodniczański Institute of Nuclear Physics, Poland*
[2] *Cracow University of Technology, Production Engineering Institute, Poland*

Corresponding author:
Jacek Jaworski
Polish Academy of Sciences
The Henryk Niewodniczański Institute of Nuclear Physics
Radzikowskiego 152, 31-342 Kraków, Poland
phone: (+48) 788 636 122
e-mail: jacek.jaworski@ifj.edu.pl

Received: 3 June 2015
Accepted: 10 July 2015

Abstract
In recent years the 3D printing methods have been developing rapidly. This article presents researches about a new composite consisted of golden and magnetite nanoparticles which could be used for this technique. Preparation of golden nanoparticles by laser ablation and their soldering by laser green light irradiation proceeded in water environment. Magnetite was obtained on chemical way. During experiments it was tested a change of a size of nanoparticles during laser irradiation, surface plasmon resonance, zeta potential. The obtained golden – magnetite composite material was magnetic after laser irradiation. On the end there was considered the application it for 3D printing devices, water filters and four-valued non-volatile memories.

Keywords
gold, magnetite, nanoparticle, ablation, laser nanosoldering method, four-valued memory, non-volatile memory, quaternary numeric system, filter.

Introduction

In recent years the 3D printing methods have been developing rapidly. They are used to quickly fabricate a model of a physical part or assembly. Usually three-dimensional computer aided design (CAD) is used for production prototypes [1] but also there exist 3D printing devices controlled manually. The 3D printing processes are used in different branches of life from printing of bio-ceramic implants for human body [2] to houses.

There are three main methods of 3D printing:

- *Stereolithography* (SLA) – additive creating process using liquid UV-curable photopolymer and a UV laser to build parts layer after layer. On each layer, the laser beam traces a part cross-section pattern on the surface of the liquid photopolymer and solidifies the pattern traced on the polymer and adheres it to the layer below. After that the SLA's elevator platform is descended by a single layer thickness, typically 0.05 [mm] to 0.15 [mm], fresh liquid polymer covers the solidified shape and the process is repeated with a new cross-section [3],
- *Selective Laser Sintering* (SLS) – technique fusing small particles of plastic, metal, ceramic, or glass powders into a mass that has a desired 3-dimensional shape by using a high power laser. The laser selectively fuses powdered material by scanning cross-sections on the surface of a powder bed. After each cross-section is scanned, the powder bed is lowered by one layer thickness, a new layer of material is applied on top, and the process is repeated until the part is completed [4],

- *Laser Engineered Net Shaping* (LENS) – a technology of fabrication metal parts by using a metal powder injected into a molten pool created by a focused, high-powered laser beam. The laser is used to melt metal powder fed coaxially into the focus of the laser beam through a deposition head. The focused laser beam passes through the center of the head. The X-Y table moves under the motionless head creating a certain layer. Next the head is moved up vertically to the table and the next layer is created [5].

These methods work with a typical resolution of tenths of millimeter, rarely hundredths. The work presented below focuses on materials consisted on nanoparticles which could be used to construct more fine prototypes by 3D printing devices than it is possible in current devices. Nanoparticles – particles with diameter not bigger than 100 [nm] – have been present on Earth since the beginning of its existence as a result of volcanic eruption, erosion or other natural processes. Currently they are produced, as by-products during industrial processes and are usually treated as air pollution, which should be removed from atmosphere because of their adverse impact on health [6–9]. However even in the early history of human civilization (5 century B.C.) multiscale particles were applied to produce color glass and ceramics. Later during the medieval period they were used in the fabrication of stained glass and more recently for photographic materials [10, 11]. Today this class of materials is of interest to researchers and engineers because of their potential applications.

Metal nanoparticles suspended in a solution exhibit different optical, magnetic and electrical properties from bulk materials [12, 13]. They could be used as a catalyst whose activity is dependent on the size of particles [14]. Nanoparticles have much more gainful ratio an area of surface to volume than microparticles and bulk materials thanks to it they could be more effective catalysts per mass unit. In recent years gold nanoparticles were paid much attention of material scientists because of its application in biotechnology [15–17]. Gold is harmless and firmly combines with compounds possessing biochemical functions such as polypeptides, DNA [18–20].

There are many various methods of manufacturing nanoparticles, from chemical way [21, 22], combustion [23] to pulverization [24] and mechanical communition by milling or by electrical discharge [25–27].

In general there are two main kinds of the manufacturing based on the "bottom up" approach consisting in growing nanoparticles atoms by atoms [10] or by reduction of bulk material into nanoparticles called "top down" approach [10].

Experiments presented in the paper focused on production new composites owing two kinds of nanoparticles. Successful nanosoldering of two metals: gold and cobalt was already reported by Swiatkowska et al. [28]. Metal – metal oxide nanosoldering was presented in a paper of Kawaguchi et al. [29]. Researches presented in this work continue and develop Kawaguchi's researches testing behavior of gold and magnetite particles with extending irradiation time, their shape, optical properties, stability and zeta potential [30]. This work presents golden and magnetite nanoparticles with new optical and magnetic properties with the special emphasis on manufacturing a new medium for 3D printing devices – the method of production of spatial objects by systematic addition of successive layers of material of the specified shape, with higher resolution then currently used. Also there are presented potential application of the new material and the manner of their implementation.

Production of golden and magnetite nanoparticles

Golden nanoparticles were obtained on a laser ablation process in water. The process removed small liquid drops of metal from a solid surface by irradiating it with a laser beam. Generally during the ablation process at low laser flux, the material is heated by the absorbed laser energy and evaporates or sublimates. At high laser flux, the material is typically converted to a plasma. Usually, laser ablation refers to removing material with a pulsed laser, but it is possible to ablate material with a continuous wave laser beam if the laser intensity is high enough.

For experiments described in the article gold nanoparticles were prepared by pulsed laser ablation in liquid (PLAL). Gold metal plate (> 99.99 [%]) [31] was placed on the bottom of glass vessel filled with 5 [cm^3] of deionized water and ablated by 1064nm wavelength pulsed beam of a neodymium doped yttrium aluminium garnet (Nd:YAG) laser Quanta – ray GCR – 170 operating at 10 [Hz] at the laser energy 100 [mJ/pulse]. The laser spot diameter on the gold surface was 1 [mm] (laser fluence 13 [J/(cm^2· pulse)]) [32]. A Scuentech AC2501 power meter was used to monitor the laser power.

The ablation process was held in the device shown in Fig. 1. A vessel with an immersed in water golden plate was situated on a rotating table. The rotation of the golden plate reduced a negative effect of cavities creation by the laser beam which lowered efficien-

cy of nanoparticles creation process. Another adverse effect is a creation of a cloud of golden nanoparticles above the golden plate which scatters the laser light. A reason of the cloud creation is a laser beam melt gold in a certain point of the plate and sputter golden droplets around the point. They pass some distance from the point and stop creating the torus-shaped cloud. A stirrer shown in Fig. 1 was used to dissipate the clouds. Thermodynamic process of the metal ablation was described by Tran X. Phuoc and Minking K. Chyu [33].

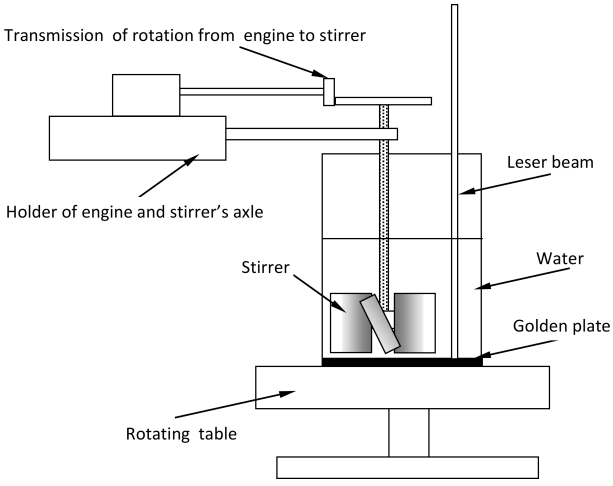

Fig. 1. A scheme of laser ablation process.

The first step of the experiment was determination of an average diameter of nanoparticles and their concentration in suspension produced in the same conditions at the same time. Concentration of golden particles was measured by inductively coupled plasma optical emission spectrometry (ICP-OES). Average diameters of gold nanoparticles was measured by non-invasive back scatter method based on dynamic light scattering of Zetasizer Nano ZS of Malvern company and confirmed by Scanning Electron Microscope (SEM) and also Transmission Electron Microscope (TEM).

Zetasizer measurements showed the average diameter of golden nanoparticles as 57.1 [nm] with the full-width at half maximum (FWHM) of Gaussian peak 23.1 [nm]. It meant that we could assumed the average diameter as 57 [nm] with the standard deviation ±10 [nm]. SEM observations confirmed it. The concentration of gold in solution grows linearly with the ablation time. The result of the concentration of golden nanoparticles dependent on time is shown in Fig. 2. For further studies 10 minutes ablation time was chosen arbitrary for preparation gold nanoparticles. During particles diameter measurement by Zetasizer zeta potential was also measured. Just after production it was – 36 (±6) [mV].

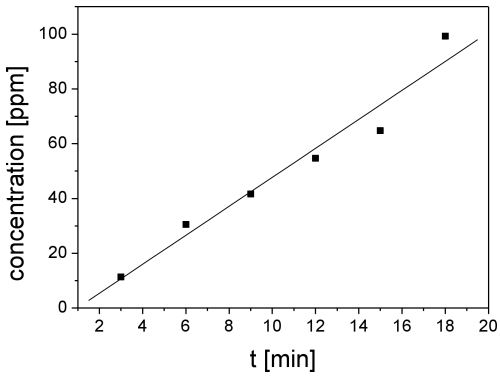

Fig. 2. Dependence of a gold nanoparticle concentration on the ablation time measured by inductively coupled plasma optical emission spectrometry (ICP-OES).

For testing stability of golden solution it was also measured next day, two days after and three days after preparation. The size was stable, it means coagulation did not occurred. Zeta potential decreased next day to – 44 [mV] and was stable for next days. Suspensions with zeta potential between – 30 to – 40 [mV] present moderate stability but below – 40 [mV] – good stability.

Magnetite nanoparticles were obtained on a chemical way from mixing $FeCl_3 \cdot 6H_2O$ and $FeCl_2 \cdot 4H_2O$ with NaOH in water [34]. Fe_3O_4 solutions were produced with four concentrations: 0.01 [g/dm^3], 0.02 [g/dm^3], 0.04 [g/dm^3]. After preparation two groups of particles for all solutions were obtained. First group had a diameter from 100 to 140 [nm] and the second on – from 500 to 600 [nm]. TEM observation shoved that magnetite nanoparticle size was from a few to over a dozen nanometers. Measured diameters have not changed during next 2 days. This result showed that magnetite nanocrystals agglomerated to big stable complexes just during chemical creation of magnetite. Zeta potential measured just after magnetite production showed value around 23 [mV] for all three samples which indicated incipient instability. After two days great differences occurred between them. The sample with magnetite concentration 0.01 [g/dm^3] presented – 60 [mV] zeta potential, 0.02 [g/dm^3]: – 43 [mV] and [0.04 g/dm^3]: – 22 [mV]. It illustrated that two first solutions obtained achieved good stability but the third one was still unstable.

Laser irradiation

A. Golden particles

In a first step of experiments with nanosoldering pure gold nanoparticles were irradiated. The 4 [ml] deionized water was mixed with 1 [ml] gold nanopar-

ticles suspension with 48 [ppm] (0.053 [%]), prepared as it was described above and next the suspension was irradiated by a pulsed laser beam with the wavelength of 532 [nm], frequency 10 [Hz] and fluence of 2.5 [J/(pulse·cm^2)] during 3, 6, 12, 24, 48, 96 minutes. The green light (532 [nm]) was used to induce surface plasmon resonance (SPR) [34] on surfaces of golden particles. The effect could be described as a collective oscillation of surface electrons stimulated by a light beam [35, 36]. During the experiment the colour of the suspension changed with irradiation time from red to grey which pointed out decreasing of green light absorption in the suspension. An ultraviolet-visible spectroscopy (UV-Vis) measurements confirmed this simple observation. The Fig. 3 shows a typical optical transmission spectrum of the virgin and the laser irradiated solutions prepared by the UV-Vis device.

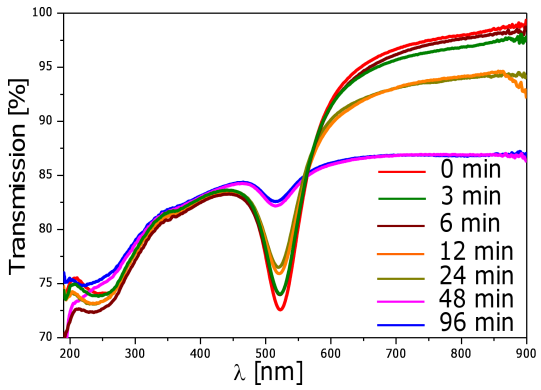

Fig. 3. Optical transmission spectrum of gold nanoparticle suspension before irradiation and irradiated during 3, 6, 12, 24, 48 and 96 minutes.

Positions of a plasmon minima are in a range between 514.5 to 522.5 [nm] and a wavelength of plasmon minimum decreases with increasing of an ablation time. In a time range between 0 to 48 minutes, decreasing of plasmon wavelength is almost linear (Fig. 4a). Over this range the plasmon wavelength still decreases but slower. The figure 4b shows the transmission plasmon wavelength minimum height normalized to the size independent transmission at $\lambda = 400$ [nm]. After 48 minutes of irradiation the SPR practically disappeared.

Papers [36, 37] relate changing of a position of plasmon wavelength with changing of diameter of nanospheres. According to the papers decreasing of plasmon wavelength with the irradiation time in the Fig. 4 suggests decreasing of gold nanospheres' diameter with elongation of irradiation time. Link and El-Sayed [36] shows a nanoparticle size dependence on the adsorption plasmon wavelength maximum position. The wavelength of SPR grew with the nanosphere's diameter growth. Similar analysis was performed by Kreibig and Genzel [37] for gold nanoparticles, and they also found this same dependence.

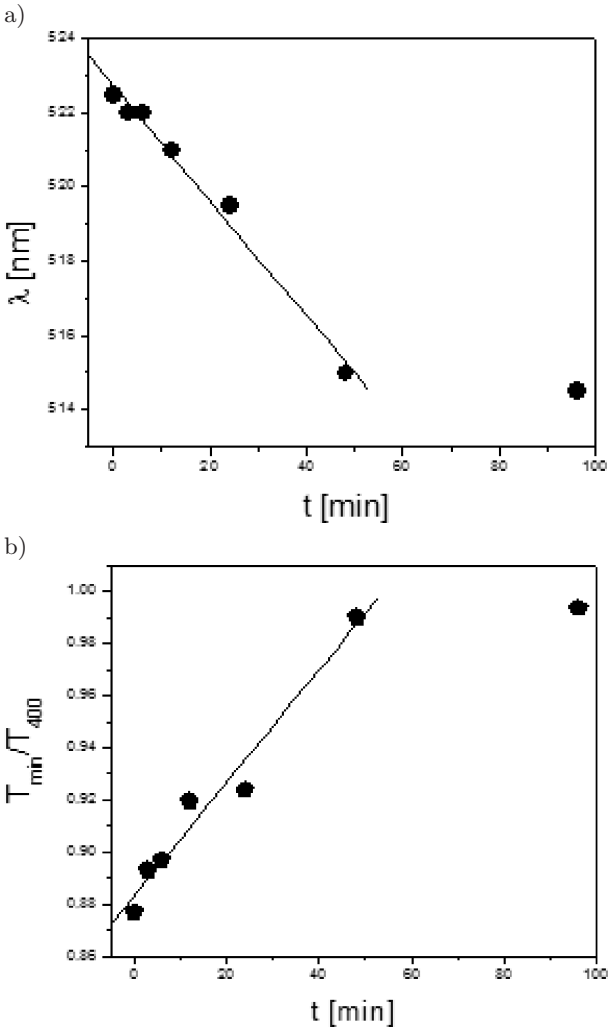

Fig. 4. a) plasmon wavelength as a function of irradiation time of gold nanoparticles suspension before irradiation and irradiated during 3, 6, 12, 24, 48 and 96 minutes; b) the transmission plasmon wavelength minimum height normalized to the size independent transmission at $\lambda = 400$ nm for gold nanoparticle suspension as a function of time

The Fig. 4b shows the transmission plasmon wavelength minimum height normalised to the size independent transmission at $\lambda = 400$ nm. The ratio increases almost linear from 0 to 48 minutes of irradiation and next increases still but only a little. The depth of plasmon minimum diminishes and colour of suspension changes from red to grey with elongation of irradiation time. The behaviour could suggest decreasing of gold nanospheres' number in the suspension and creation other forms of gold nanopar-

ticles because of melting of gold nanoparticles under influence of green laser light. Microscopic observations confirmed our suggestions. Changing shape of nanoparticles and creation nanonetworks with irradiation time is shown in Fig. 5. After irradiation time between 0 to 6 [min] the gold suspension consisted of separated gold nanoparticles with average size about 50 [nm] but observed values were ranged from 10 to 90 [nm]. After 12 [min] of irradiation time new structures have been formed – gold clusters consisted of hundreds gold nanospheres. After 24 [min] of irradiation time nanowires among nanoparticles were created. The nanowires connected 40–80 [nm] diameter nanospheres. Number of nanospheres was reduced compared to initial gold suspension. After 48 [min] of irradiation nanospheres occurred very rarely and their size was decreasing to 45 [nm] and 30 [nm] after 96 [min]. It was only a few nanospheres bigger than 45 [nm] This behaviour was in accordance with Mafune [10] and Kurita [38] results.

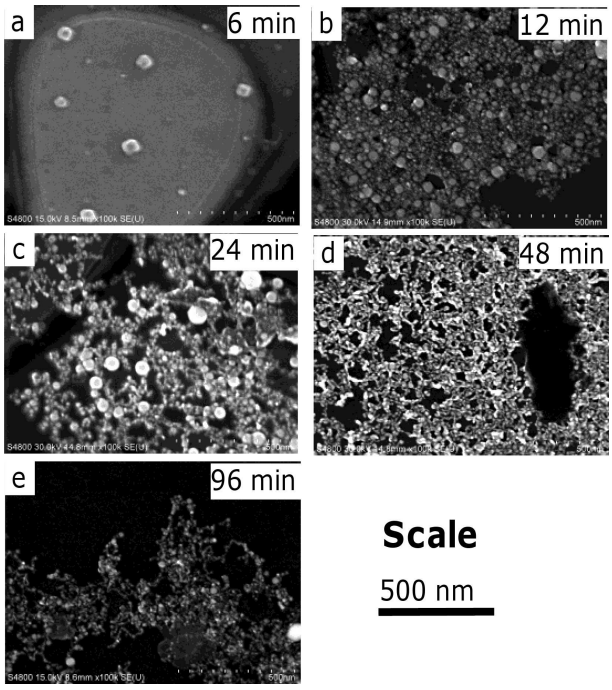

Fig. 5. SEM images of gold nanoparticles irradiated during: a) 6, b) 12, c) 24, d) 48 and e) 96 minutes. Magnification – 100 000.

The change of the nanoparticle suspension colour from red to grey could be explained by transformation of the suspension of separated gold nanospheres, which presents good plasmon absorption, to the suspension consisted of a small number of gold nanospheres with a reduced diameter interconnected by nanobridges creating an irregular structure similar to nanocobweb. The nanocobweb did not reveal the surface plasmon resonance.

The creation of the nanocobweb could be explained by the attraction between nanospheres surfaces molten by oscillating electrons on particle's surface (Fig. 6). Free gold nanoparticles (Fig. 6a) are irradiated by short pulse of laser beam (Fig. 6b). Surface electrons interact with laser light, absorb its energy and use the energy for their collective motion on the surface what causes melting of an outer part of gold nanosphere, leaving a solid core. If two nanoparticles are close enough to each other van der Waals interaction can create a bridge between particles (Figs. 6c and 6d).

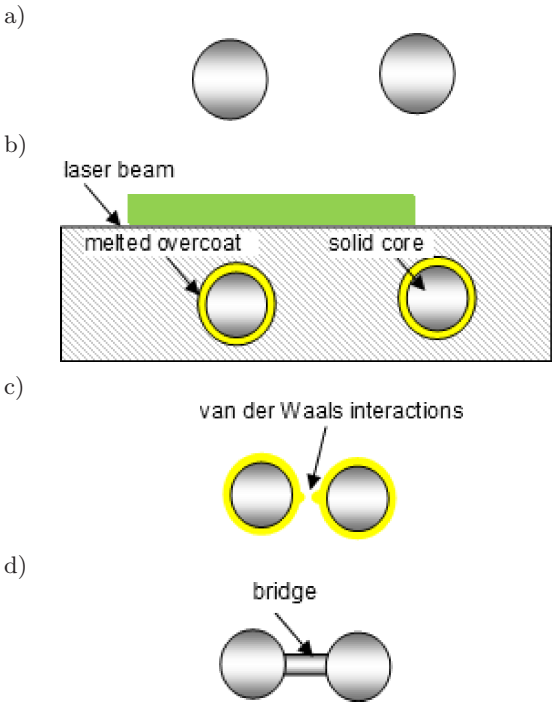

Fig. 6. Nanobridges creation: a) free gold nanoparticles, b) surface of gold nanoparticles melted by laser beam, c) van der Waals interactions start creation of nanobridge from melted overcoat of nanosphere, d) bridge created.

Because of the fast heat flow from nanospheres to the water the time of bridge creation is comparable to a laser pulse duration and the number of laser pulses (time of irradiation) is very important for creation of the nanostructure like the cobweb. The laser beam was narrow compared to vessel diameter and a small number of pulses cannot satisfy the conditions of nanocobweb creation (Fig. 5a). But, according to Bernoulli law of large numbers, if the number of laser pulses is big enough conditions of nanocobweb creation occur in all suspension After 96 minutes irradiation nanoshells were created (Fig. 7).

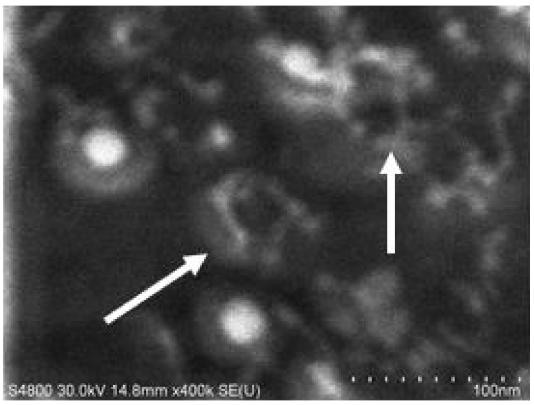

Fig. 7. Gold nanoparticles irradiated 96 minutes. Magnification – 400.000. Arrows point nanoshells.

The nanoshells were created from groups of nanoparticles which melted and created bridges among themselves. Brownian motion and bridges creation lead to nanoshells and nanorings formation. A two dimensional simple model of nanoring creation is shown in the Fig. 8. Free nanospheres (Fig. 8a) are irradiated by green laser beam and create nanobridges among themselves (Fig. 8b). Brownian motion moves single nanospheres and interconnect them by brigdes, collect them near bigger structure which is analogous to "condensation nuclei" and next laser pulses create next bridges among structures creating nanoclusters which could be in a form of nanoshells as well (Fig. 8c) [39].

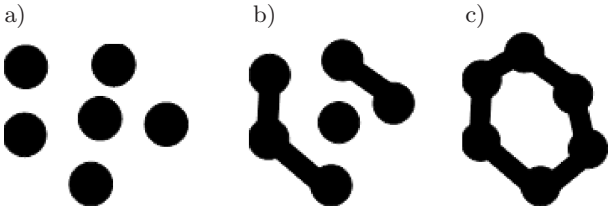

Fig. 8. Two dimensional simple model of nanoring creation: a) group of nanoparticles before irradiation, b) during irradiation nanobridges are created and nanoclusters due to nanobridges, c) Brownian motion moves nanoclusters, they collects and nanorings are created during irradiation.

B. Magnetite particles

Pure magnetite was also tested for nanosoldering. Solution of 0.02 [g/l] Fe_3O_4 prepared on chemical way was irradiated by a pulsed laser beam with the wavelength of 532 [nm], frequency 10 [Hz] and fluence of 2.5 [J/(pulse·cm^2)] during 3, 6, 12, 24, 48, 96 minutes under same conditions as gold nanospheres. In contrast to gold, the colour of the magnetite suspension did not change with irradiation time. After the irradiation an optical transmission spectrum were obtained which did not show differences among different irradiation time (Fig. 9).

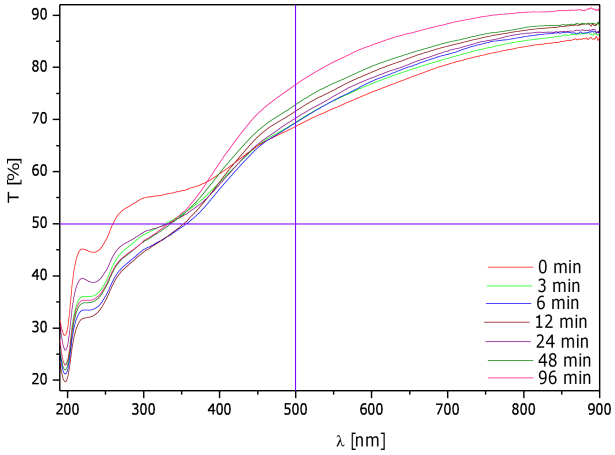

Fig. 9. Optical transmission spectrum of magnetite nanoparticle suspension before irradiation and irradiated during 3, 6, 12, 24, 48 and 96 minutes.

Also the magnetite suspensions were analyzed by TEM images and electron diffraction patterns which did not show differences what suggest that laser irradiation laser beam 532 [nm] wavelength does not influence on magnetite properties. Average diameter of magnetite nanoparticle measured by TEM was 8 [nm] – much smaller than average size of golden nanospheres. The Fig. 10 shows TEM pictures of magnetite before and after 48 minutes of irradiation. Also TEM diffraction did not indicate any changes

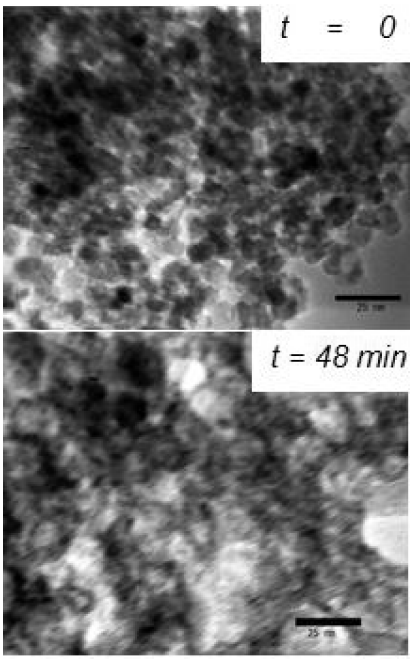

Fig. 10. TEM pictures of magnetite before and after 48 minute of irradiation. Magnitude – 600 000.

during the irradiation. The Fig. 11 shows the diffraction picture of non-irradiated and irradiated magnetite. Before and during irradiation the suspension of magnetite was shook and mixed so its zeta potential changed from −12 [mV] after shaking to +8 [mV] after 96 minutes irradiation.

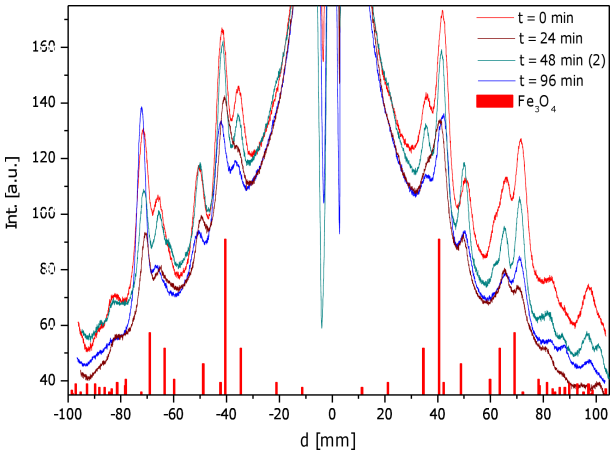

Fig. 11. TEM diffraction spectra of magnetite non-irradiated and irradiated for 24, 48 and 96 minutes.

C. Goldden and magnetite particles

Experiments with welding of gold and magnetite started from tests in macroscale. The test was based on melting gold and next connecting it with solid magnetite. The experiment was successful. The Fig. 12 shows result of welding gold and magnetite in macroscale. Welding did not destroy magnetic properties of magnetite. Successful welding magnetite with gold in macroscale suggested soldering possibility in nanoscale.

Fig. 12. A gold piece welded with magnetite in argon atmosphere.

In nanosoldering experiment of gold – magnetite nanoparticles the 4 [ml] 0.01 [%] (A) and 0.02% water solution of Fe_3O_4 was mixed with 1 [ml] gold nanoparticles suspension with 48 [ppm] (0.053 [%]) with an average diameter 60 [nm] of gold nanospheres and irradiated with a pulsed laser having the wavelength of 532 [nm] and fluence rate of 2.5 [J/(pulse · cm^2)] during 3, 6, 12, 24, 48, 96 minutes. The colour of the suspension changed with irradiation time from red to grey. Figure 13 shows a typical optical transmission spectrum of the virgin and the laser irradiated A solutions. As shown in the Fig. 13 positions of optical transmission spectrum minima are inclosed in a range between 523.5 and 528.5 [nm] and decrease with increasing of an ablation time and vanish beyond 24 minutes of ablation time.

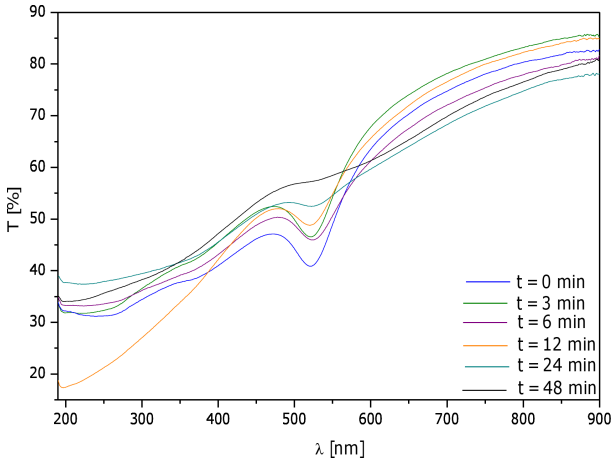

Fig. 13. Optical transmission spectrum of gold nanoparticles with magnetite mixture without irradiation and irradiated during 3, 6, 12, 24, 48 and 96 minutes.

For B solution the minimum vanished after 6 minutes of ablation time.

Colour of samples irradiated with lengthening time changed from red to grey, Fig. 14.

Magnetic particles of suspensions irradiated 96 minutes and non-irradiated were collected by permanent magnet, extracted from the solution and observed by TEM. The Fig. 15 presents cross-section spectra of electron diffraction pictures of these two suspensions. Peaks of the sample without irradiation represent pure magnetite but in the spectrum of the sample irradiated 96 minutes maxima represent both gold and magnetite. This proves a physical connection between the golden and magnetite nanoparticles in the suspension irradiated 96 minutes.

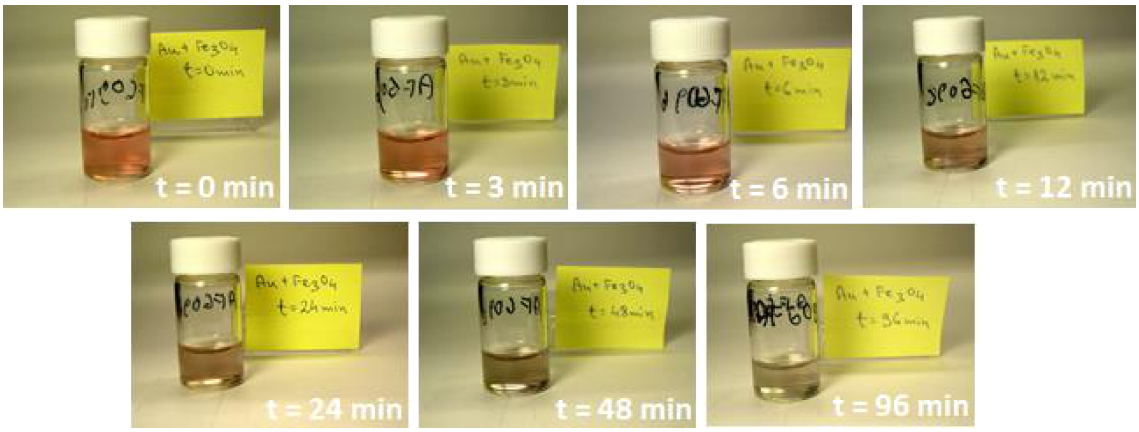

Fig. 14. Suspensions of gold nanoparticles mixed with magnetite without irradiation and irradiated during 3, 6, 12, 24, 48 and 96 minutes.

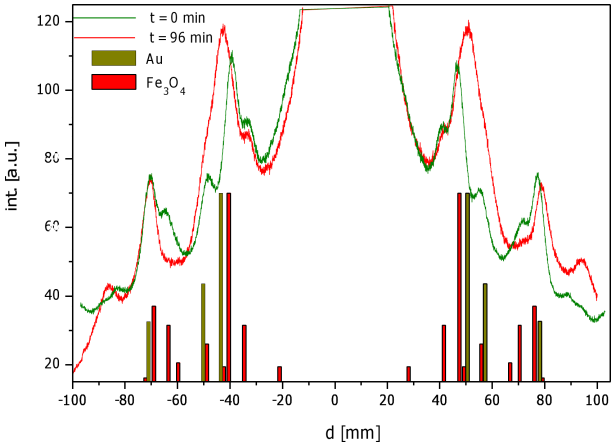

Fig. 15. Cross-section spectra of electron diffraction pictures for irradiation time 0 and 96 minutes after magnetic extraction. The green curve represents the suspension before irradiation, the red curve represents the suspension after 96 minutes irradiation and red bars show theoretical magnetite maxima and green bars – gold maxima.

Differences in structures of nanoparticles in both suspensions shows TEM pictures (Fig. 16). The left picture presents mixture of gold and magnetite nanoparticles but on the right picture a golden sphere with magnetite inclusions is demonstrated which could belong to group of materials called Matrix-Dispersed Nanoparticles [39].

These results proved that the irradiation transformed the gold – magnetite suspension to a new kind of structures which possess features of both components, what means it was magnetic and presented surface plasmon resonance under certain conditions.

Zeta potential of irradiated suspensions turned to positive value when exposure time was longer than 6 minutes. But during the re-measurement after two days it decreased again to negative value.

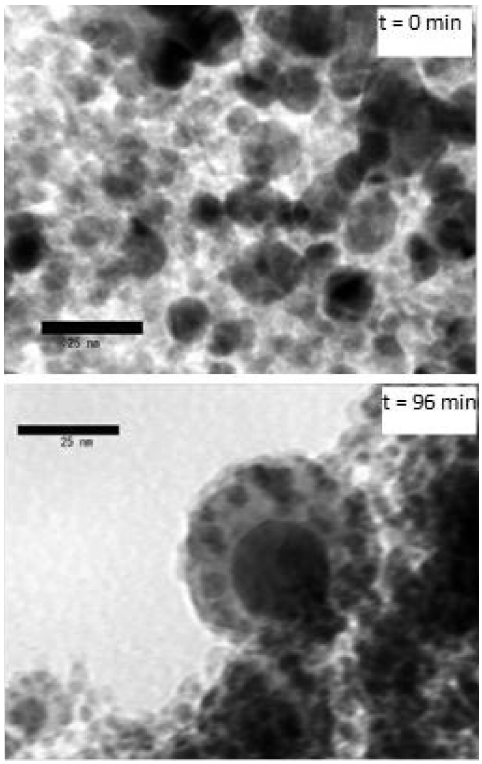

Fig. 16. Gold – magnetite suspensions non-irradiated and irradiated 96 min. Magnification – 800 000.

Potential applications

Magnetite is already applied in filters for uptake magnetic particles for liquid. Also magnetite was tested to adsorb fatty acids from solutions like oleic from hexane [40]. The new golden – magnetite material could be used in new kind of filters for these substances. Viruses and other water pollutions have negative zeta potential. Particles with positive zeta

potential are used for capture them from a water. The golden – magnetite composite had positive zeta potential after irradiation. If would be possible to keep this potential long time what make it possible to use this material in a new kind of water filters.

Gold and magnetite are harmless for human body so their composite could be used as a medicine carrier [41] or because its positive zeta potential could be medicine by itself collecting around viruses or bacteria and applied magnetic field with high frequency would be causing of high oscillations of magnetite increasing local temperature and kill bacteria and viruses. The proper shape of golden magnetite composite could be obtained by 3D micro – printing device. There are already known methods of micro and nano-focusing laser beam [42–45] which could be used in nano- or micro- 3D printers. 3D printing device could use micro-focused laser beam for sinter magnetite and gold to the appropriate shape.

Many programmable devices need a non-volatile memory (read only memory RAM) like a washing machine, TV set or dishwasher. This kind of memory could be realized using 3D printing of gold nanoparticles or gold nanoparticles with magnetite. The idea of recording is presented in the Fig. 17. The nano-dispenser of golden nanoparticles puts them on a tin plate. The laser beam solders golden nanoparticles to thin substrate. Using a binary system "0" could be fulfilled as free space and "1" as a golden chain. For reading information the tin plate with soldered nanoparticles could be illuminated by green light micro-beam. The tin plate will reflect the beam but in golden particles will oscillate electrons in SPR absorbing light. It will be observed full reflection for "0" but for "1" – part of green light will be absorbed. For saving space it could be used different system than the binary – ternary or quaternary. In nature the most common numerical system for recording data is the quaternary system. It is used in deoxyribonucleic acid (DNA) and ribonucleic acid (RNA) in which the genetic information is recorded by using four nucleobases [46].

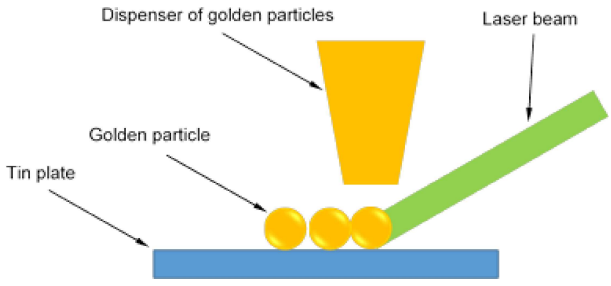

Fig. 17. Scheme of 3D printing device for golden non-volatile memory.

If nature have used the system billions of years it means it is the most effective. The 3D printing device can reproduce the numerical system in the non-volatile memory. It can print nothing for "0", line for "1", cross for "2" and circle for "3". The characters are different and easy to distinguish for the reading system. As in the binary numerical system the basic unit of information is "bit" which represents "0" or "1" so in the quaternary system it could be called "quat" representing 0, 1, 2, 3. Another way to record data in the quaternary system is presented in the Fig. 18.

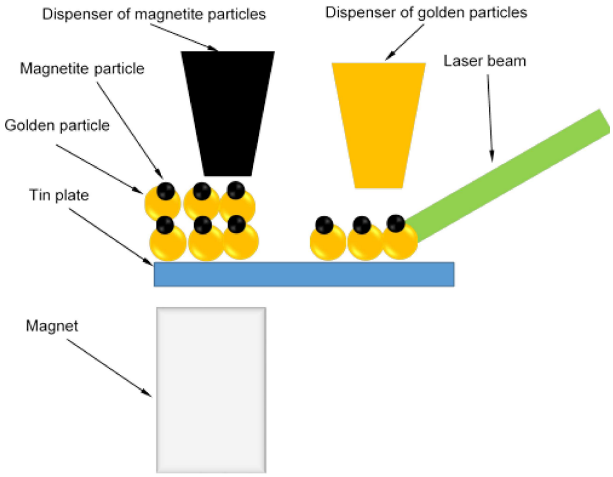

Fig. 18. Scheme of 3D printing device for golden- magnetite non-volatile memory.

The idea of the recording is similar to presented in the Fig. 17. The nano-dispenser of golden nanoparticles puts them on the tin plate and the laser beam solders golden nanoparticles to thin substrate. Next the nano-dispenser of magnetite nanoparticles covers golden particle by magnetite ones and the magnetic field from the magnet organizes magnetic moments of magnetite nanoparticles. The laser beam solders them. Depending on a number of repetitions golden and magnetite layer or their lengths or widths defined "quats" will be represented.

These two examples do not show all possibilities of data recording by 3D nano-printing device using golden and magnetite nanoparticles. There are much more possibilities to achieve this goal.

Conclusions

Experiments confirmed that during green laser beam irradiation, the diameter of gold nanoparticles decreased with irradiation time and the particles melting created a nanonetwork of gold nanospheres

connected by nanowires. The longer irradiation time the smaller golden nanoparticles and more nanowires occurred. Also light reflection of these structures changed with elongation of irradiation time. In contrast, magnetite was not sensitive for green laser beam generally, but the irradiation time influenced on zeta potential of magnetite nanoparticles suspension. The irradiation of gold and magnetite mixture formed the new kind of structure which was magnetic, its zeta potential was positive for some cases and optical properties changed with lengths of irradiation time. The results provide possible applications of a new approach of 3D nano-printing method which could be used for printing new medicines, water and other liquids filters and new kinds of non-volatile memories.

Jacek Jaworski, PhD and Grzegorz Gawłowski, MSc Eng. thank prof. Naoto Koshizaki, prof. Takashi Sasaki, Kenji Kawaguchi, PhD and Yoshie Ishikawa, PhD for their scientific support.

References

[1] Chua C.K., Leong K.F., Lim C.S., *Rapid prototyping: principles and applications*, World Scientific Publishing Co. Pte. Ltd., Singapore, 2nd edition, 135, 2003.

[2] Vorndran E., Moseke C., Gbureck U., *3D printing of ceramic implants*, MRS Bulletin, 40, 127–136, 2015.

[3] Hull C.W., *Apparatus for production of three-dimensional objects by stereolithography*, Patent US4575330 A, published 11 March 1986.

[4] Deckard C., *Method and apparatus for producing parts by selective sintering*, U.S. Patent 4,863,538, published 5 September 1989.

[5] Justin D.F., Stucker B.E., Gabbita D.J.R., Britt D.W., *Laser based metal deposition (LBMD) of antimicrobials to implant surfaces*, Patent US20110208304 A1, published 25 August 2011.

[6] Davison R.L., Natusch D.F.S, Wallace J.R., Evans C. Jr, *Trace Elements in Fly Ash. Dependence of Concentration on Particle Size*, Environmental Science & Technology, 8, 13, 1107–1113, 1974.

[7] Smith R.D., Campbell J.A., Nielson K.K., *Characterization and Formation of Submicron Particles in Coal-Fired Plants*, Atmos. Environ., 13, 607–617, 1979.

[8] Huang S.-L.., Hsu M.-K.., Chan C.-C.., *Effects of submicrometer particle compositions on cytokine production and lipid peroxidation of human bronchial epithelial cells*, Environmental Health Perspectives, 111, 4, 478–482, 2003.

[9] Smith R.D., Campbell J.A., Nielson K.K., *Characterization and Formation of Submicron Particles in Coal-Fired Plants*, Atmos. Environ., 13, 607–617, 1979.

[10] Hornyak G.L., Tibbals H.F., Dutta J., Moore J.J., *Introduction to Nanoscince and Nanotechnology*, CRC Press, Taylor & Francis Group, Broken Sound Parkaway NW, 14–19, 2009

[11] Sharma V., Park K., Srinivasarao M., *Colloidal dispersion of gold nanorods: Historical background, optical properties, seed-mediated synthesis, shape separation and self-assembly*, Mater. Sci. Eng. R Rep., 65, 1–38, 2009.

[12] Mafuné F., Kohno J., Takeda Y., Kondow T., Sawabe H., *Formation of gold nanoparticles by laser ablation in aqueous solution of surfactant*, J. Phys. Chem. B 105, 5114–5120, 2001.

[13] He S., Yao J., Jiang P., Shi D., Zhang H., Xie S., Pang S., Gao H., *Formation of Silver Nanoparticles and Self-Assembled Two-Dimensional Ordered Superlattice*, Langmuir, 17, 5, 1571–1575, 2001.

[14] Takami A., Yamada H., Nakano K., Koda S., *Size Reduction of Silver Particles in Aqueous Solution by Laser Irradiation*, Jpn. J. Appl. Phys., 35, 6B, L781–L783, 1995.

[15] Zhang Y., Zhang J., *Controllable microstructure of Au nanoparticle-DNA oligonucleotide conjugates*, Journal of Chemical and Pharmaceutical Research, 6, 4, 255–259, 2014.

[16] Storhoff J.J., Lazaorides A.A., Mucic R.C., Mirkin C. A., Letsinger R.L., Schatz G.C., *What Contrals the Optical Properties of DNA-Linked Gold Nanoparticles Assembles?*, J. Am Chem. Soc., 122, 4640–4650, 2000.

[17] Ren L., Chow G.M., *Synthesis of NIR-sensitive Au-Au_2S nanocolloids for drug delivery*", Mater. Sci. Eng. C, 23, 113, 2003.

[18] Nuzzo R.G., Allara D.L., *Adsorption of bifunctional organic disulfides on gold surfaces*, J. Am. Chem. Soc, 105, 4481–4483, 1983.

[19] Brust M., Walker M., Bethel D., Schiffrin D.J., Whyman R., *Synthesis of thiol – derivatised gold nanoparticles in a two-phase liquid – liquid system*, J. Chem. Soc., Chem. Commun., 7, 801–802, 1994.

[20] Kiang C.H., *Phase transition of DNA – linked gold nanoparticles*, Physica A, 321, 164–169, 2003.

[21] Wei H., Li B., Du Y., Dong S., Wang E., *Nucleobase – metal hybrid materials: preparation of submicrometer-scale, spherical colloidal particles of adenine-gold(III) via a supramolecular hierarchical self-assembly approach*, Chem. Mater., 19, 12, 2987–2993, 2007.

[22] Bardhan R., Wang H., Tam F., Halas N.J., *Facile Chemical Approach to ZnO Submicrometer Particles with Controllable Morphologies*, ACS J. Surf. Coll., Langmuir, 23, 5843–5847, 2007.

[23] Hernández N., González-González V.A., Dzul-Bautista I.B., Cienfuegos-Pelaes R.F, *Characterization and magneticproperties of NdXBi1-XFe0.95Co0.05O3 nanopowders synthesized by combustion-derived method at low temperature*, Journal of Magnetism and Magnetic Materials, 377, 466–471, 2015.

[24] Zhuang Y., Biswas P., *Submicrometer Particle Formation and Control in a Bench-Scale Pulverized Coal Combustor*, Energy & Fuels, 15, 3, 510–516, 2001.

[25] Delaportas D., Svarnas P., Alexandrou I., Siokou A., Black K., Bradley J.W., *γ-Al2O3 nanoparticle production by arc-discharge in water: in situ discharge characterization and nanoparticle investigation*, J. Phys. D: Applied Physics, 42, 24, 245204, 2009.

[26] Ashkarran A.A., Irajizad A., Mahdavi S.M., Ahadian M.M., Nezhad M.R.H., *Rapid and efficient synthesis of colloidal gold nanoparticles by arc discharge method*, Applied Physics, A96, 2, 423–428, 2009.

[27] Jaworski J.A., Fleury E., *Sub-Micrometer Particles Produced by a Low-Powered AC Electric Arc in Liquid's*, JNN, 12, 1, 604–609, 2012.

[28] Świątkowska-Warkocka Ż, Koga K., Kawaguchi K., Wang H., Pyatenko A., Koshizaki N., *Pulsed laser irradiation of colloidal nanoparticles: a newsynthesis route for the production of non-equilibrium bimetallic alloy submicrometer spheres*, RSC Advances, 3, 79–83, 2013.

[29] Kawaguchi K., Jaworski J., Ishikawa Y., Sasaki T., Koshizaki N., *Preparation of Gold/Iron Oxide Composite Nanoparticles by a Laser-Soldering Method*, IEEE Transactions on magnetics, 42, 10, 3620–3622, 2006.

[30] Keck C.M., *Cyclosporine Nanosuspensions: Optimised Size Characterisation & Oral Formulations*, Inaugural-Dissertation zur Erlangung des akademischen Grades des Doktors der Naturwissenschaften (Dr. rer. nat.) eingereicht im Fachbereich Biologie, Chemie, Pharmazie der Freien Universität Berlin, 221–232, 2006.

[31] Mafuné F., Kohno J., Takeda Y., Kondow T., *Formation of Gold Nanonetworks and Small Gold Nanoparticles by Irradiation of Intense Pulsed Laser onto Gold Nanoparticles*, J. Phys. Chem. B, 107, 46, 12589–12596, 2003.

[32] Kawaguchi K., Jaworski J., Ishikawa Y., Sasaki T., Koshizaki N., *Preparation of gold/iron-oxide composite nanoparticles by a unique laser process in water*, Journal of Magnetism and Magnetic Materials, 310, 2369–2371, 2007.

[33] Phuoc T.X., Chyu M.K., *Synthesis and Characterization of Nanocomposites Using the Nanoscale Laser Soldering in Liquid Technique*, Journal of Materials Science & Nanotechnology, 1, 1, 1–5, 2013.

[34] Jaworski J., Gawłowski G., *Production and properties of composite material comprising Gd multiscale particles*, Management and Production Engineering Review, 6, 1, 16–20, 2015.

[35] Link S., El-Sayed M.A., *Shape and size dependence of radiative, non-radiative and photothermal properties of gold nanocrystals*, Int. Reviews in Physical Chemistry, 19, 3, 409-453, 2000.

[36] Link S, El-Sayed M.A., *Spectral properties and relaxation dynamics of surface plasmon electronic oscillations in gold and silver nanodots and nanorods*, J. Phys. Chem. B, 103, 8410–8426, 1999.

[37] Kreibig U., Genzel L., *Optical absorption of small metallic particles*, Surface Science, 156, 2, 678–700, 1985.

[38] Kurita H., Takami A., Koda S., *Size reduction of gold particles in aqueous solution by pulsed laser irradiation*, Applied Physics Letters, 72, 7, 789–791, 1998.

[39] Świątkowska-Warkocka Ż., Jaworski J.A., *Synthesis, Characterization and Applications of Nanocomposite Particles*, book *Nanotechnology*, Vol.2: *Synthesis and Characterization*, Studium Press LLC, 2013.

[40] Korolev V.V., Ramazanova A.G., Yashkova V.I., Balmasova O.V., Blinov A.V., *Adsorption of fatty acids from solutions in organic solvents on the surface of finely dispersed magnetite: 1. Isotherms of adsorption of oleic, linoleic, and linolenic acid from carbon tetrachloride and hexane*, Colloid Journal, 66, 6, 700–704, 2004.

[41] Zhou H., Lee J., Park T.J., Lee S.J., Park J.Y., Lee J., *Ultrasensitive DNA monitoring by Au-Fe_3O_4*

nanocomplex, Sensors and Actuators B, 163, 224–232, 2012.

[42] Takahara J., Yamagishi S., Taki H., Morimoto A., Kobayashi T., *Guiding of a one-dimensional optical beam with nanometer diameter*, Opt. Lett., 22, 7, 475–477, 1997.

[43] Nikolov I. D., Kurihara K., Goto K., *Nanofocusing probe optimization with anti-reflection coatings for a high-density optical memory*, Nanotechnology, 14, 9, 946–954, 2003.

[44] Choi H., Pile D.F.P., Nam S., Bartal G., Zhang X., *Compressing surface plasmons for nano-scale optical focusing*, Opt. Ex., 17, 9, 7519–7524, 2009.

[45] Oulton R.F., Sorger V.J., Zentgraf T., Ma R.-M., Gladden C., Dai L., Bartal G., Zhang X., *Plasmon lasers at deep subwavelength scale*, Nature, 461, 629–632, 2009.

[46] Watson J.D., Crick F.H.C., *Molecular Structure of Nucleic Acids: A Structure for Deoxyribose Nucleic Acid*, Nature, 171, 4356, 737–738, 1953.